Appl. Phys. B 26, 23–30 (1981)

Applied Physics

Influence of the Source Bandwidth on the Observation of Microwave Photon Echoes

F. Rohart and B. Macke

Laboratoire de Spectroscopie Hertzienne, Associé au C.N.R.S., Université de Lille I, F-59655 Villeneuve d'Ascq Cedex, France

Received 20 March 1981/Accepted 5 May 1981

Abstract. The fluctuations of the source frequency are shown to be responsible of an extra damping of the optical precession and of the photon echoes observed in the experiments involving many shots and an averaging of the detected signals. Assuming a phase diffusing model and various profiles for the frequency power spectrum, the r.m.s. accumulated phase error is calculated and two asymptotic behaviours are pointed out according to the relative values of the sequence duration and of the frequency correlation time. The calculation is well supported by a photon echo experiment at a 3-mm wavelength.

PACS: 42.50, 42.65 G.

Recently there has been a growing interest of the theoreticians in the effects of the source bandwith on the resonant interaction of a strong field with an ensemble of 2-level systems [1]. These works include line saturation, ac Stark splitting, etc.... and have been stimulated by experiments on resonance fluorescence [2] and double optical resonance [3]. Most of these studies have concentrated on the steady state limit and, if we except a paper related to the time-dependent spectrum of fluorescence [4] and another one [5] evoking incidentaly the optical precession (free induction decay), the theoretical works concerning the coherent transients induced by a noisy source are restricted to the optical nutation (Rabi oscillations) [6–10]. However there is a considerable experimental interest in optical precession and in photon echoes for the development of ultrahigh resolution spectroscopy with non monochromatic sources [11, 12]. In a single-shot experiment only the source frequency fluctuations for the sequence duration have indeed to be considered. It was recently claimed that the natural linewidth $1/T_2$ is reached with a laser which remains stable during T_2 for the optical precession (nearly steady state preparation) and only during the resonant $\pi/2-\pi$ pulses for the photon echoes (instead of during the scan time for saturation spectroscopy) [12]. These rather qualitative predictions are well supported by two recent experiments on solid-state samples [11, 12]. The coherent transients observed in gases [13, 14] are weaker and single-shot experiments are generally unfeasible owing to problems of signal to noise ratio. In this case, the optical precession and the photon echoes are usually detected as a beat with the incident field (heterodyne technique) [13, 14] and their observation requires an averaging on many shots. The source bandwidth involves then an extra-damping of the averaged transients which is examined in the present paper. This study is not purely academic and was originated from T_2 measurements in the millimetre range, anomalous decay rates of photon echoes having been observed [15].

The arrangement of our paper is as follows. In Sect. 1, Bloch-Maxwell equations, including frequency fluctuations, are derived and their solutions are outlined for the optical precession, the 2 and 3 pulse photon echo sequences. In Sect. 2, the results are specialized to a particular model of phase diffusing source, assuming different profiles for the frequency power spectrum: according to the source spectral properties, the frequency fluctuations are shown to lead to reversible or

0340-3793/81/0026/0023/$01.60

irreversible dephasings. These dephasing processes are compared to those resulting from the molecular motions (space and/or velocity diffusion). The experiment at a 100-GHz frequency is described in Sect. 3: the frequency power spectra of two different sources are measured and are used to predict the relative amplitudes of the echoes obtained with these two sources, in good agreement with the actual observation. The main results are summarized in Sect. 4 (conclusion) where the interest of microwave experiments in order to develop models for laser experiments is pointed out.

1. General Background

In order to restrict this paper to the effects due to the source bandwidth, we consider a gas of 2-level systems (hereafter referred to as molecules), through which a linearly polarized plane wave propagates in the z-direction: the gas absorption frequency can be switched in or out of resonance [13, 14] (e.g. by Stark switching technique), while the incident field $E(0,t)$ is continuously applied. The amplitude fluctuations of $E(0,t)$ during the optical precession are efficiently reduced by the averaging procedure and they do not affect the optical nutation in so far as their relative value remains small, a condition fulfilled by the fairly good sources considered here. They are then neglected and we take

$$E(0,t)=\tfrac{1}{2}E_0\exp\{i[\omega t+\Phi(t)]\}+\text{c.c.}, \tag{1}$$

where $\Phi(t)$ is a real random variable describing the phase fluctuations of the incident field [10] and is obviously related to the source frequency fluctuations, the instantaneous frequency being $\omega+\dot{\Phi}(t)$. Throughout this paper, the frequency deviation $\dot{\Phi}(t)$ is assumed to be a stationary, Gaussian, centred random variable, whereas the phase $\Phi(t)$ may be diffusing (for careful definitions, see e.g. [16]). Introducing the so-called instantaneous rotating frame [4], the field and the gas polarization in the cell $(0<z<l)$ are written as

$$E(z,t)=\tfrac{1}{2}\tilde{E}(z,t)\cdot\exp\{i[\omega t-kz+\Phi(t)]\}+\text{c.c.}, \tag{2}$$

$$P(z,t)=\tfrac{1}{2}\tilde{P}(z,t)\cdot\exp\{i[\omega t-kz+\Phi(t)]\}+\text{c.c.}, \tag{3}$$

where $\tilde{E}(z,t)$, $\tilde{P}(z,t)$, $\exp[i\Phi(t)]$ are complex functions varying slowly in time compared to $e^{i\omega t}$ and in space compared to $\exp(-ikz)$. k is the propagation constant ω/c. Within this slowly varying amplitude approximation [17], assuming the gas to be optically thin and neglecting the propagation duration l/c across the l long cell, the Bloch-Maxwell equations for a particular v_z molecular velocity class become (in S.I. units)

$$\frac{dn}{dt}=-\frac{\mathrm{i}E_0}{2\hbar}(\tilde{P}-\tilde{P}^*)-(n-n_0)/T_1, \tag{4}$$

$$\frac{d\tilde{P}}{dt}=-\mathrm{i}\frac{\mu^2E}{\hbar}n+\mathrm{i}[\omega_0+kv_z-\omega-\dot{\Phi}(t)]\tilde{P}-\tilde{P}/T_2, \tag{5}$$

$$|\tilde{E}(l,t)|^2=E_0^2-\frac{\mathrm{i}\omega l}{2\varepsilon_0 c}(\tilde{P}-\tilde{P}^*)E_0, \tag{6}$$

where ω_0 is the molecular eigenfrequency, μ is the transition dipole matrix element (assumed to be real), n is the difference of level populations per unit volume, n_0 its value at equilibrium and T_1 (resp. T_2) is the phenomenological relaxation time of population (resp. coherence). $|\tilde{E}(l,t)|^2$ is proportional to the signal delivered by a quadratic detector placed at the cell termination. Using the Stark switching technique, we are only interested in its time dependent part proportional to (1/i) $(\tilde{P}-\tilde{P}^*)$, obviously always real.
In the following, this quantity is calculated in the case of the 3-pulse photon echo experiment [15] discussed in Sect. 3, corresponding to a truncated Carr-Purcell sequence [18] (see the related Stark sequence in Fig. 1). The results regarding the optical precession and the conventional photon echo experiment will be obviously included. Postponing the corresponding discussion, the resonant $\pi/2$ and π-pulses are provisionaly assumed to be very short and ideally efficient for all the velocity classes, that is:
i) starting from the equilibrium $(n=n_0)$, the $\pi/2$-pulse creates the maximum gas polarization $(\tilde{P}=-\mathrm{i}\mu n_0)$ and equalizes the level populations $(n=0)$
ii) the π-pulses invert the populations $(n\to-n)$ and change the polarization in its complex conjugate $(\tilde{P}\to\tilde{P}^*)$, reversing the inhomogeneous dephasing process. Between the resonant pulses, the molecules are far off resonance and the gas polarization due to the velocity class v_z evolves freely according to the equation

$$\frac{d\tilde{P}}{dt}=\mathrm{i}[\omega_0+kv_z-\omega-\dot{\Phi}(t)]\tilde{P}-\tilde{P}/T_2 \tag{7}$$

and thus

$$\tilde{P}(v_z,t)=\tilde{P}(v_z,t_0)\cdot\exp[\mathrm{i}(\omega_0+kv_z-\omega)(t-t_0)]\cdot\exp[-(t-t_0)/T_2]\cdot\exp\{-\mathrm{i}[\Phi(t)-\Phi(t_0)]\}, \tag{8}$$

where $\Phi(t)-\Phi(t_0)$ is the phase increment during the interval (t_0,t). After integrating on the Doppler profile,

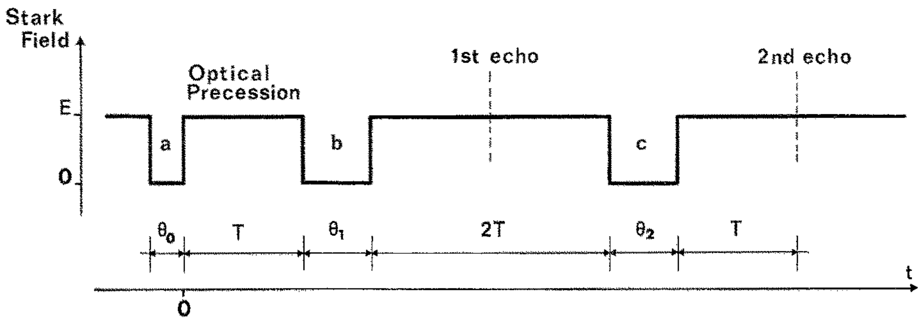

Fig. 1a–c. Stark sequence used for the observation of 3 pulse-photon echoes: (a) $\pi/2$ pulse (b) and (c) π pulses. The pulse durations, assumed to be negligible ($\theta_0, \theta_1 \ll T$), are enlarged for sake of visibility

we easily obtain:
– for the optical precession following the $\pi/2$ pulse ($0<t<T$):

$$\begin{aligned}(1/i)[\tilde{P}(t)-\tilde{P}^*(t)]\\ &= -2\mu n_0 \exp(-t/T_2)\cdot\exp(-k^2 v_0^2 t^2/4)\\ &\quad\cdot\cos[(\omega_0-\omega)t-\Phi(t)+\Phi(0)]\,,\end{aligned} \tag{9a}$$

– for the first echo ($T<t<3T$):

$$\begin{aligned}(1/i)[\tilde{P}(t)-\tilde{P}^*(t)]\\ &= +2\mu n_0 \exp(-t/T_2)\cdot\exp[-k^2 v_0^2 (t-2T)^2/4]\\ &\quad\cdot\cos[(\omega_0-\omega)(t-2T)-\Phi(t)+2\Phi(T)-\Phi(0)]\,,\end{aligned} \tag{9b}$$

– for the second echo ($t>3T$):

$$\begin{aligned}(1/i)[\tilde{P}(t)-\tilde{P}^*(t)]\\ &= -2\mu n_0 \exp(-t/T_2)\cdot\exp[-k^2 v_0^2 (t-4T)^2/4]\\ &\quad\cdot\cos[(\omega_0-\omega)(t-4T)-\Phi(t)+2\Phi(3T)\\ &\quad-2\Phi(T)+\Phi(0)]\end{aligned} \tag{9c}$$

where v_0 is the most probable velocity. The two exponentials appearing in (9) correspond obviously to the homogeneous and inhomogeneous dampings, the latter being removed at the time of the photon echoes ($t=2T, 4T$). The last term may be generally written as $\cos[(\omega_0-\omega)(t-2nT)+\varphi(t)]$ with $n=0, 1, 2$. As usual [13], the polarization appears as a beat between the cw source field and the field reemitted by the gas at its eigenfrequency ω_0. This beat is here affected by the source noise, its instantaneous frequency being $\omega_0-\omega-\dot{\Phi}(t)$. In a single shot experiment, this involves only some fluctuations in the beat frequency. On the contrary, if an averaging on many shots is required, the statistical mean of $\cos[\omega_0-\omega)\,(t-2nT)+\varphi(t)]$ has to be made over all the various initial times. Owing to the gaussian character of $\Phi(t)$ [and then of $\varphi(t)$], we get

$$\begin{aligned}&\langle\cos[(\omega_0-\omega)(t-2nT)+\varphi(t)]\rangle\\ &=\cos[(\omega_0-\omega)(t-2nT)]\exp[-\tfrac{1}{2}\langle\varphi^2(t)\rangle]\,,\end{aligned} \tag{10}$$

where $\langle\varphi^2(t)\rangle$ is the variance of the accumulated phase error which can generally be derived from the frequency power spectrum $S_{\dot{\Phi}}$ of the source [19]. $\mathrm{Exp}[-\langle\varphi^2(t)\rangle/2]$ describes obviously the extra damping resulting from the source noise and the averaging. At this point and before an explicit calculation of this term, let us emphasize we are interested here in the extra damping of the optical precession and of the photon echoes due to the source fluctuations but neither in the exact process of the inhomogeneous damping (spatial or Doppler, pulses preparing a particular molecular class or not, etc....) nor in the absolute magnitude of the corresponding coherent transients. From this point of view, most of the rather drastic approximations made previously may be relaxed and we have only to examine how far the effects of the frequency fluctuations, not considered previously, are actually negligible. The most relevant parameter for this discussion is obviously the r.m.s. frequency deviation $\sigma_{\dot{\Phi}}$ and it is sufficient that $\sigma_{\dot{\Phi}}$ is much smaller than the Rabi frequency $\omega_1=\mu E_0/\hbar$. When the pulses prepare a particular molecular class, this condition ensures that this class is well defined and in particular does not change from one pulse to another. If the pulses are not selective, this condition involves that the instantaneous Rabi frequency $(\omega_1^2+\dot{\Phi}^2)^{1/2}$ is nearly equal to ω_1 and that the efficiency of the $\pi/2$ and π pulses is constant. In the following, the condition $\sigma_{\dot{\Phi}}\ll\omega_1$ is assumed to hold, a relation well fulfilled in our experiment.

2. Calculation of the Accumulated Phase Error

For a single precession starting at the time t_0, the accumulated phase error at the time t_0+t is

$$\Phi(t_0+t)-\Phi(t)=\int_{t_0}^{t_0+t}\dot{\Phi}(\theta)d\theta \tag{11}$$

and its variance $\langle\varphi^2(t)\rangle$ calculated on many shots is then simply the square of the r.m.s. phase deviation $\sigma_{\Phi}(t)$ during the time t

$$\langle\varphi^2(t)\rangle=\langle[\Phi(t_0+t)-\Phi(t_0)]^2\rangle=\sigma_{\Phi}^2(t)\,. \tag{12}$$

Let us introduce the frequency autocorrelation function $R_{\dot{\Phi}}(\tau)$ and its power spectrum[1] $S_{\dot{\Phi}}(\Omega)$ with

$$S_{\dot{\Phi}}(\Omega)=\int_{-\infty}^{+\infty} R_{\dot{\Phi}}(\tau)\,\mathrm{e}^{-\mathrm{i}\Omega\tau}d\tau\,, \tag{13}$$

$$R_{\dot{\Phi}}(\tau)=\frac{1}{2\pi}\int_{-\infty}^{+\infty} S_{\dot{\Phi}}(\Omega)\,\mathrm{e}^{\mathrm{i}\Omega\tau}d\Omega\,. \tag{14}$$

$\sigma_{\Phi}^2(\tau)$ is easily expressed as [19]

$$\sigma_{\Phi}^2(\tau)=\tau\int_{-\infty}^{+\infty} S_{\dot{\Phi}}(\Omega)\,\mathrm{sinc}^2(\Omega\tau/2)d(\Omega\tau/2\pi) \tag{15}$$

with $\mathrm{sinc}\,x=\sin x/x$. The phase diffusion of the source is conveniently characterized by a phase diffusing time τ_D [20] such as

$$\sigma_{\Phi}(\tau_D)=1\ \mathrm{Rd}\,. \tag{16}$$

Calculations similar to those leading to (15) allow us to derive the variances $\langle\varphi^2(2T)\rangle$ and $\langle\varphi^2(4T)\rangle$ of the accumulated phase error at the time of the first and second echoes. We get

$$\langle\varphi^2(2T)\rangle=4\sigma_{\Phi}^2(T)-\sigma_{\Phi}^2(2T)\,, \tag{17}$$

$$\begin{aligned}\langle\varphi^2(4T)\rangle=\sigma_{\Phi}^2(4T)-4\sigma_{\Phi}^2(3T)\\ +4\sigma_{\Phi}^2(2T)+4\sigma_{\Phi}^2(T)\,.\end{aligned} \tag{18}$$

Equations (12), (15), (17), and (18) show clearly that the extra-damping of the optical precession and of the photon echoes due to the source fluctuations can be derived from the measured frequency power spectrum. However some general features can be derived from the knowledge of $S_{\dot{\Phi}}(0)$ and of the r.m.s. frequency deviation $\sigma_{\dot{\Phi}}$ only, with

$$\sigma_{\dot{\Phi}}^2=\langle\dot{\Phi}^2\rangle=R_{\dot{\Phi}}(0)=\frac{1}{2\pi}\int_{-\infty}^{+\infty} S_{\dot{\Phi}}(\Omega)d\Omega\,. \tag{19}$$

In particular, the long term behaviour is obtained by considering the sinc^2-function appearing in (15) as peaked at $\Omega=0$ and we get

$$\sigma_{\Phi}^2(\tau)=S_{\dot{\Phi}}(0)\tau\,. \tag{20}$$

This law is characteristic of the irreversible limit in the theory of Brownian motion [6] and most of the calculations in laser theory are made within this limit. From (17) and (18) we derive for $\langle\varphi^2(2T)\rangle$ and $\langle\varphi^2(4T)\rangle$ expressions identical to (20) with $\tau=2T$ and $4T$, respectively: in the irreversible limit the influence of the frequency noise depends only on the sequence duration. Physically one may say that the frequency changes during the pulse sequence are so numerous that, by no means, an echo rephasing can be obtained. On the other hand, the short term behaviour is obtained by putting $\mathrm{sinc}^2(\Omega\tau/2)=1$ in (15). Using (19), we get

$$\sigma_{\Phi}^2(\tau)=\sigma_{\dot{\Phi}}^2\tau^2 \tag{21}$$

and, from (14) and (15)

$$\langle\varphi^2(2T)\rangle=\langle\varphi^2(4T)\rangle=0\,. \tag{22}$$

At this order of approximation, there is a damping of the optical precession but an exact rephasing at the time of the echoes, a behaviour characteristic of the so-called reversible limit [6]. The damping of the echoes appears obviously at a higher order in time but its calculation requires a detailed knowledge of $S_{\dot{\Phi}}(\Omega)$, as also the calculation of the r.m.s. phase deviation $\sigma_{\Phi}(\tau)$ for arbitrary values of τ. For three different profiles $S_{\dot{\Phi}}(\Omega)$, Table 1 gives the frequency autocorrelation function $R_{\dot{\Phi}}(\tau)$, the variances of the phase deviation $\sigma_{\Phi}^2(\tau)$ calculated in the general case, of the accumulated phase errors $\langle\varphi^2(2T)\rangle_{\mathrm{rev}}$ and $\langle\varphi^2(4T)\rangle_{\mathrm{rev}}$ at the time of the first and second echoes, calculated in the reversible limit, at the lowest non zero order. $1/q$ is the frequency correlation time and fixes the frontier between the reversible ($q\tau\ll 1$) and irreversible ($q\tau\gg 1$) limits, where $q\tau$ may be interpreted as the mean number of frequency jumps occuring during the time interval τ. The Lorentzian profile, associated to a Poissonian distribution of the frequency jumps, is commonly used in laser theory but some difficulties arise in the definition of the random variable $\ddot{\Phi}$, useful to discuss precisely the effects of the frequency fluctuations during the resonant pulses. These difficulties are avoided by the gaussian profile, leading to a better convergence of the involved integrals. At least, the exponential profile is introduced in Table 1 since it fits very well our experimental spectrum (Sect. 3).

The results concerning the damping of the first and second echoes in the reversible limit ($q\tau\ll 1$) deserve some comments. For the same sequence overall duration, the effects of the frequency noise are weaker on the 2nd echo than on the 1st one, the multipulse sequences, as well known, reducing the dephasing processes [18]. However the same t^3 dependence is obtained for $\langle\varphi^2(2T)\rangle$ and $\langle\varphi^2(4T)\rangle$ with a Lorentzian profile. On the contrary, in the case of the two other profiles, a t^4 law is obtained for the 1st echo and, most important feature, there is a nearly perfect rephasing at the time of the 2nd echo ($qt\ll 1$) with a residual variance $\langle\varphi^2(t)\rangle\sim t^6$. This example shows that an exact knowledge of the power spectrum $S_{\dot{\Phi}}(\Omega)$ is required for a good prediction of the short term behaviour of coherent transients.

[1] $S_{\dot{\Phi}}(\Omega)$ has to be carefully distinguished from the field power spectrum which is the Fourier transform of the autocorrelation function of $E(0,t)$.

Table 1. Theoretical results concerning the three considered profiles of the frequency power spectrum

Profile	Lorentzian	Gaussian	Exponential
$S_\Phi(\Omega)$	$\frac{2\sigma_\Phi^2}{q}\frac{1}{1+\Omega^2/q^2}$	$\frac{\sigma_\Phi^2\sqrt{2\pi}}{q}\exp(-\Omega^2/2q^2)$	$\frac{\sigma_\Phi^2\pi}{q}\exp\left(-\left\lvert\frac{\Omega}{q}\right\rvert\right)$
$R_\Phi(\tau)$	$\sigma_\Phi^2\exp(-q\lvert\tau\rvert)$	$\sigma_\Phi^2\exp(-q^2\tau^2/2)$	$\sigma_\Phi^2\frac{1}{1+q^2\tau^2}$
$\sigma_\Phi^2(\tau)$	$(2\sigma_\Phi^2/q^2)\,[q\tau-1+\exp(-q\tau)]$	$\sigma_\Phi^2\tau^2\left\{\frac{\sqrt{2\pi}}{q\tau}\operatorname{erf}\left(\frac{q\tau}{\sqrt{2}}\right)\right.$	$(\sigma_\Phi^2/q^2)\,[2q\tau\,\mathrm{Arc}\,tg\,(q\tau)$
		$\left.-\frac{2}{q^2\tau^2}[1-\exp(-q^2\tau^2/2)]\right\}$	$-\mathrm{Log}(1+q^2\tau^2)]$
$\langle\varphi^2(t)\rangle_{\mathrm{rev}}$ for $t=2T$	$q\,\sigma_\Phi^2\,t^3/6$	$\sigma_\Phi^2\,q^2\,t^4/16$	$q^2\,\sigma_\Phi^2\,t^4/8$
$\langle\varphi^2(t)\rangle_{\mathrm{rev}}$ for $t=4T$	$q\,\sigma_\Phi^2\,t^3/24$	$3\,\sigma_\Phi^2\,q^4\,t^6/1024$	$3\,\sigma_\Phi^2\,q^4\,t^6/128$

The effects discussed before can be compared to those due to the molecular diffusion, in space [21, 18, 22] or in velocity [23, 24]. There is a strong difference between these effects and those due to source fluctuations since the former lead to an instantaneous detuning $(\omega-\omega_0)$ which is *frequency* diffusing instead of *phase* diffusing for the latter and the corresponding results cannot be generally compared. This is obvious in the case of spatial diffusion in nuclear magnetic resonance where, in the same irreversible limit, the frequency diffusion leads to a phase variance proportional to t^3 [18, 22] instead of t for a phase diffusing field, (20). The difference is not so clear in the experiments of photon echoes involving velocity changing collisions, the Doppler width being much larger than the homogeneous one [23, 24]. The asymptotic behaviours of $\langle\varphi^2(2T)\rangle$ at the echo time seem identical to those obtained previously with a Lorentzian profile for $S_\Phi(\Omega)$ ($\sim t^3$ at short term, $\sim t$ at long term). The explanation, however, is quite different since these experiments never take place in the irreversible limit $\Gamma t \gg 1$ (Γ: rate of velocity changing collisions) and since the elastic collisions are characterized by a r.m.s. frequency jump $k\Delta u$ (Δu: r.m.s. velocity change) whereas only the resulting r.m.s. frequency deviation σ_Φ can be defined for the phase diffusing field. The transition from the t^3-regime to the t-regime is then related to the value of the r.m.s. phase deviation ($k\Delta ut \gtrsim 1$), not to a passage from the reversible to the irreversible limit ($\Gamma t \gtrsim 1$) [23].

3. Experiment

3.1. General

To check the previous calculations, an experiment of photon echoes was undertaken at a 3-mm wavelength on the $(J, |KM|=1, 1\to 2, 1)$ transition of methyl fluoride CH_3F ($\omega/2\pi \simeq 102$ GHz) [25]. The mm source was phase locked at the line frequency and the molecular absorption was switched off-on by a Stark technique [13, 14] (linear Stark effect). An inhomogeneous Stark field was used in order to speed up the damping of the optical precession without affecting the nutation pulses for which the Stark field is null [22]. The cell used was described elsewhere [15]. The molecular free flight across the inhomogeneous Stark field involves a reduction of the first echo but the second echo is unaffected in the even Carr-Purcell sequence [15] previously discussed (Fig. 1) and used in the experiment. A similar technique was proposed to overcome convection effects on spin echoes [18]. The required Stark sequence was delivered by a Stark generator (0–75 V, rise time 20 ns) driven at a 2.5-kHz rate by a 20-MHz clock. The detection included a Schottky barrier mixer, a wide band (1 kHz–100 MHz) video amplifier and a 256 channel digital averager (channel width $\geqq 10$ ns). The overall sequence duration was typically 10 μs (sample pressure $\simeq 1$ mTorr). The mm-wave was provided directly by a klystron phase locked on a 4–5 GHz frequency standard, denoted A or B. A was a 2–4.2 GHz klystron also phase locked on a 15 MHz cristal oscillator (Microwave System MOS-1) and B was a 4.8–5.3 GHz solid-state oscillator (C.T.I. A-5317) phase locked on a 100–110 MHz synthetizer (Adret 6100). A and B are nearly equivalent for uses in conventional spectroscopy but we shall see they lead to quite different results in time resolved spectroscopy.

3.2. Characterization of the Source Fluctuations

The amplitude fluctuations of a microwave oscillator are usually negligible [26] and only the frequency

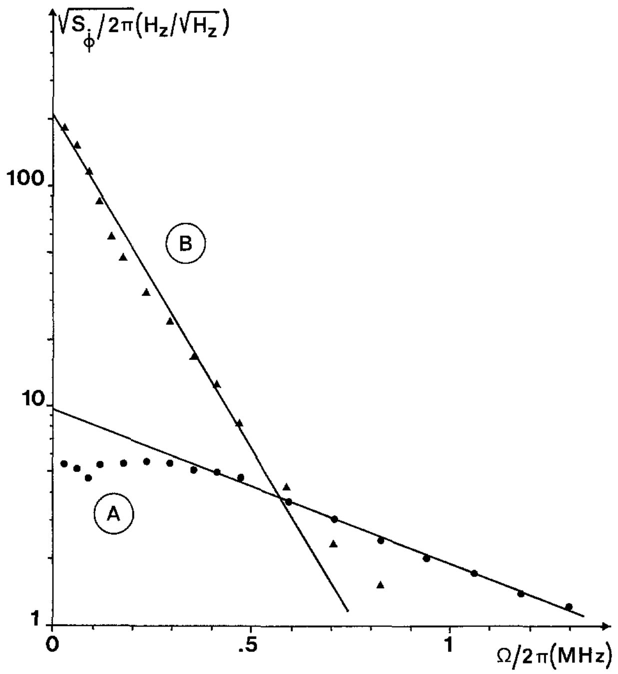

Fig. 2. Semi-logarithmic representation of the frequency power spectrum $(S_\Phi/2\pi)^{1/2}$ of the mm-source phase locked on the A and B frequency standards. The points are derived from the experimental spectra and the full straight lines correspond to the exponential spectra used in the calculations (see text)

Table 2. Parameters characterising the frequency noise of the mm-source phase locked on the A and B frequency standards, within the model of a S_Φ exponential profile. τ_D is the phase diffusing time corresponding to a r.m.s. phase deviation of 1 Radian

Frequency standard	$[S_\Phi(0)/2\pi]^{1/2}$	$q/2\pi$	$1/q$	$\sigma_\Phi/2\pi$	τ_D
A	9.5 Hz/$\sqrt{Hz}$	310 kHz	0.51 μs	3.0 kHz	1.8 ms
B	210 Hz/$\sqrt{Hz}$	71 kHz	2.2 μs	32 kHz	5.9 μs

fluctuations are considered here. The frequency power spectrum S_Φ was recorded by the following technique. The mm-wave was sent on a Fabry-Perot resonator [27] detuned from resonance by a half-width of its resonance curve ($\simeq 1$ MHz) and acting as a frequency discriminator. The output mm-wave was detected and the resulting amplitude noise was used to modulate a high-quality signal supplied by a synthetizer (Ailtech 360). The latter was frequency swept around 6 MHz and its output signal was sent on a receiver tuned at 6 MHz (bandwidth $\simeq 1.7$ kHz). Except for the 0-frequency signal due to the 6 MHz-carrier, the receiver delivered a signal proportional to the spectrum $S_\Phi^{1/2}$ of the mm-source. The calibration of the whole chain was checked by applying a known frequency modulation on the mm-source. Let us note that the measured mm-frequency noise was slightly larger than when calculated from the noise characteristics of the A and B frequency standards measured by a spectrum analyzer (respectively 0.2 Hz/$\sqrt{Hz}$ and 6 Hz/$\sqrt{Hz}$ at 20 kHz from the carrier, i.e. -105 dBc/Hz and -77 dBc/Hz, dB under the carrier in a 1 Hz-bandwidth). The extra noise due to the mm-phase locking device, could however be made negligible by carefully adjusting the gain and the bandwidth of the servo loop.

Figure 2 gives the frequency power spectra of the mm-source phase locked on the A and B frequency standards in a semi-logarithmic representation. The points are derived from the experimentally recorded spectra and the full lines correspond to ideal exponential spectra. Let us recall that the very low frequency part (<2 kHz, not reported) of these spectra is perturbed by experimental artefacts and let us note moreover that, contrary to the case of steady state spectroscopy, only the frequencies $>1/2\pi t$ (t: sequence duration) has to be considered in a photon echo experiment. The A and B spectra S_Φ are clearly very different in amplitudes as well as in width. The A-spectrum leads to a characteristic phase diffusing time τ_D, (16), very long compared to our sequence duration and the mm-source may be considered in this case as perfect for our experiments. On the contrary, the B-spectrum is expected to lead to a significative reduction of the echo amplitudes. This spectrum is very well fitted by an exponential. Table 2 gives the parameters characterizing this exponential spectrum also as those of the A-spectrum for reference.

The self-consistency of the model leading to the parameters of this table was checked by measuring directly the r.m.s. frequency deviation σ_Φ proportional to the r.m.s. voltage delivered by the detector placed just behind the mm-FM discriminator (Fabry-Perot). The difference between this measurement and the result given in Table 2 is below the experimental error.

As a final comment of Table 2, let us note that the currently used approximation $qt \gg 1$ (irreversible limit) does not hold for the B-spectrum in our experimental conditions (5 μs $< t <$ 20 μs). However we are not far from this limit and the echo damping, then, does not depend strongly on the exact model of frequency power spectrum S_Φ.

3.3. Reduction of the Echo Amplitudes due to the Source Noise

Typical recordings obtained with a truncated Carr-Purcell sequence are given in Fig. 3. The full sequence (curve A, enlarged in A′), recorded with the A-frequency standard, clearly exhibits the basic features of a photon echo experiment: the echoes appear at

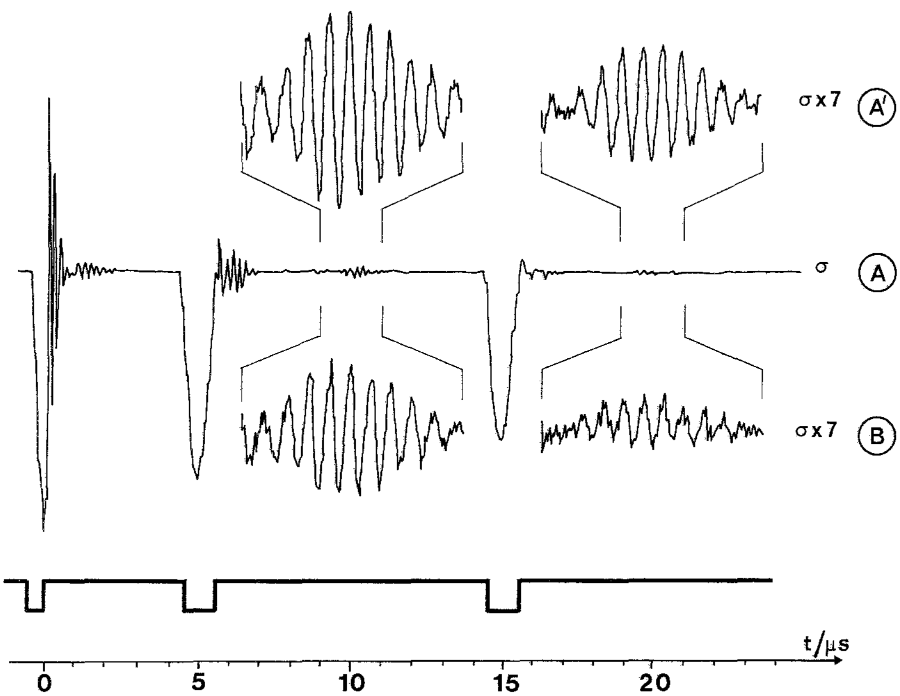

Fig. 3. Experimental evidence of the reduction of the echo amplitudes due to the source noise. This reduction is negligible with the A-frequency standard (see text) but appears clearly with the B-one. CH_3F pressure $\simeq 0.8$ mTorr, collisional broadening $\simeq 20$ kHz HWHM, Doppler broadening $\simeq 110$ kHz HWHM, Rabi frequency $\omega_1/2\pi \simeq 650$ kHz, mean Stark shift $\simeq 5.5$ MHz, Stark field inhomogeneity $\simeq 25\%$

predicted time, their sign being reversed by each π-pulse. The weak absolute magnitude of the echoes are well explained by taking into account the molecular collisions, the mm-field inhomogeneities and the molecular motions across the inhomogeneous Stark field, the latter affecting the first echo but not the second one [22, 15]. On the other hand, the noise characteristics of the mm-source in this A-case lead to a reduction of the echo amplitudes as $\exp[-\langle\varphi^2(t)\rangle/2]$ which is negligible ($<1\%$) as expected. The curve B was recorded, in the same experimental conditions, by substituting the B-frequency standard to the A-one. This entails a strong reduction of the echo amplitudes due to the corresponding larger FM noise of the mm-source. The ratio of the amplitude of the B-echo over that of the A-echo is 0.65 and 0.35 for the first and second echoes respectively. These ratios can independently derived from the source characteristics and our theoretical calculations. From Tables 1 and 2, (17) and (18), we obtain, for the extra-damping of the echoes due to the source noise

$$\exp[-\tfrac{1}{2}\langle\varphi^2(2T)\rangle] = 0.59,$$
$$\exp[-\tfrac{1}{2}\langle\varphi^2(4T)\rangle] = 0.29.$$

These values are in good agreement with the direct measurements. The same satisfactory agreement is obtained for various sequence durations and gives a kind support to the proposed model. Obviously the effects of the source noise become more and more dramatic for increasing sequence durations. For instance, in our experiment, echoes were observed for sequence durations $4T$ as long as $46\,\mu s$ with the best frequency standard whereas they become quite invisible with the other one.

Conclusion

We have examined in this paper the influence of the source bandwidth on the observation of photon echoes in experiments involving many shots and an averaging of the detected signals. The associated reduction of the echo amplitudes has been determined, assuming a phase diffusing model to describe the source field and has been explicitly calculated by taking conventional and realistic profiles for the frequency power spectrum. The asymptotic behaviours associated to the so-called reversible and irreversible limits in the theory of Brownian motion have been clearly pointed out and destinguished from the behaviours observed in experiments involving molecular diffusion processes. From an experimental point of view, our study at a millimeter wavelength has shown that two sources which are nearly equivalent in conventional steady state spectroscopy can lead to quite different results in time resolved spectroscopy. In particular, the irreversible limit approximation, well justified for calculating steady state absorption does not generally hold in a photon echo experiment. The good agreement between the measured echo amplitudes and those derived from the parameters characterizing the source noise bring a satisfactory support to the theoretical analysis.

A more systematic experimental study of the influence of the source noise requires a best characterization of the latter. Experiments on optical nutation, optical precession and photon echoes with nearly perfect mm-sources which are phase or amplitude modulated by a well defined noise are in progress in our laboratory. Such experiments are expected to bring a good insight into the corresponding phenomena in laser spectroscopy with the benefit of a negligible Doppler effect and of a more favourable time scale.

Acknowledgement. The authors wish to thank P. Rosseels for technical assistance.

References

1. A fairly comprehensive list of references may be found in a recent paper: A.T.Georges: Phys. Rev. A**21**, 2034–2048 (1980)
2. F.Y.Wu, R.E.Grove, S.Ezekiel: Phys. Rev. Lett. **35**, 1426–1429 (1975)
3. P.B.Hogan, S.J.Smith, A.T.Georges, P.Lambropoulos: Phys. Rev. Lett. **41**, 229–232 (1978)
4. J.H.Eberly, C.V.Kunasz, K.Wodkiewicz: J. Phys. B (Atom. Mol. Phys.) **13**, 217–239 (1980)
5. G.S.Agarwal: Phys. Rev. A**18**, 1490–1506 (1978)
6. K.Wodkiewicz: Phys. Rev. A**19**, 1686–1696 (1979)
7. P.Zoller: Phys. Rev. A**20**, 1019–1031 (1979)
8. A.T.Georges, P.Lambropoulos: Phys. Rev. A**20**, 991–1004 (1979)
9. J.L.F.de Meijere, J.H.Eberly: Phys. Rev. A**17**, 1416–1430 (1978)
10. J.Mostowski, K.Rzazewski: Z. Phys. B – Condensed Mater **39**, 183–185 (1980)
11. R.G.de Voe, A.Szabo, S.C.Rand, R.G.Brewer: Phys. Rev. Lett. **42**, 1560–1563 (1979)
12. R.M.MacFarlane, R.M.Shelby, R.L.Shoemaker: Phys. Rev. Lett. **43**, 1726–1730 (1979)
13. R.L.Shoemaker: *Laser and Coherence Spectroscopy*, ed. by J.I.Steinfeld (Plenum Press, New York 1978) pp. 197–371
14. R.H.Schwendeman: Annu. Rev. Phys. Chem. **29**, 537–558 (1978)
15. F.Rohart, B.Macke: 35th Symp. on Molecular Spectroscopy, Columbus, Ohio, USA (1980)
16. E.Boileau, B.Picinbono: IEEE Trans. IM**25**, 66–75 (1976)
17. C.L.Tang, B.D.Silverman: *Physics of Quantum Electronics*, ed. by P.L.Kelly, B.Lax, and P.E.Tannenwald (McGraw Hill, New York 1966) pp. 280–293
18. H.Y.Carr, E.M.Purcell: Phys. Rev. **94**, 630–638 (1954)
19. L.S.Cutler, C.L.Searle: Proc. IEEE **54**, 136–154 (1966)
20. P.Avan, C.Cohen-Tannoudji: J. Phys. B (Atom. Mol. Phys.) **10**, 155–170 (1977)
21. E.L.Hahn: Phys. Rev. **80**, 580–594 (1950)
22. P.Glorieux, J.Legrand, B.Macke: Chem. Phys. Lett. **40**, 287–291 (1976)
23. P.R.Berman, J.M.Levy, R.G.Brewer: Phys. Rev. A**11**, 1668–1688 (1975)
24. A.Flusberg: Opt. Commun. **29**, 123–125 (1979)
25. R.S.Winton, W.Gordy: Phys. Lett. **32**A, 219–220 (1970)
26. S.L.Johnson, B.H.Smith, D.A.Calder: Proc. IEEE **54**, 258–265 (1966)
27. J.Legrand, B.Segard, A.Krosta, B.Macke: Rev. Sci. Instrum. **49**, 526–530 (1978)